

# Independent Turbo Coding and Common Interleaving Method among Transmitter Branches Achieving Peak Throughput of 1 Gbps in OFCDM MIMO Multiplexing

Junichiro Kawamoto, Takahiro Asai, Kenichi Higuchi, and Mamoru Sawahashi

This paper proposes a common interleaving method associated with independent channel-encoding among transmitter antenna branches in orthogonal frequency and code division multiplexing based on multiple-input multiple-output (MIMO) multiplexing to achieve an extremely high throughput such as 1 Gbps using a 100 MHz bandwidth. This paper also investigates the average packet error rate performance as a function of the average received signal energy per bit-to-background noise power spectrum density ratio ( $E_b/N_0$ ). We found that the loss in the required average received  $E_b/N_0$  of the proposed method is only within approximately 0.3 dB in up to a 12-path Rayleigh fading channel, using 16QAM and Turbo coding with a coding rate of 5/6. We also clarify that even for a large fading correlation among antenna branches, 1 Gbps is still possible by increasing the transmission power. Therefore, the proposed method reduces the processing rate to 1/4 in the turbo decoder with only a slight loss in the required average received  $E_b/N_0$ .

**Keywords:** Broadband wireless access, multiple-input multiple-output (MIMO), channel coding, interleaving.

## I. Introduction

High-speed downlink packet access (HSDPA) based on the wideband code-division multiple-access (W-CDMA) air interface can achieve a much higher throughput than 2 Mbps with a best-effort type service by employing such key techniques as adaptive modulation and channel coding, a hybrid automatic repeat request, and fast packet scheduling [1]. However, anticipating the current and future tremendous increases in the amount of data traffic, new broadband wireless access schemes must establish broadband packet transmission with a maximum data rate above 100 Mbps in the forward link using an approximate 50 to 100 MHz bandwidth [2]-[4] (note that the target information bit rate corresponds to approximately ten fold higher than that achievable in HSDPA with a 5 MHz bandwidth). Furthermore, this broadband wireless access scheme must flexibly support isolated-cell and indoor office environments as well as cellular systems from the standpoint of further reducing the cost of radio access networks.

To develop a broadband wireless access scheme, members of our research group clarified that orthogonal frequency and code division multiplexing (OFCDM), which is originally based on multi-carrier CDMA [5], [6], or orthogonal frequency division multiplexing (OFDM) exhibits better performance than conventional direct sequence (DS)-CDMA based wireless access [2]-[4]. This is because OFCDM and OFDM mitigate the degradation caused by severe multipath interference in a broadband channel by utilizing many sub-carriers with a low symbol rate. Furthermore, members of our research group recently proposed OFCDM with variable spreading factor (VSF)

---

Manuscript received Dec. 26, 2003; revised July 30, 2004.

Junichiro Kawamoto (phone: +81 46 840 3470, email: kawamoto@mlab.yrp.nttdocomo.co.jp), Takahiro Asai (email: asai@mlab.yrp.nttdocomo.co.jp), Kenichi Higuchi (email: higuchi@mlab.yrp.nttdocomo.co.jp), and Mamoru Sawahashi (email: sawahashi@mlab.yrp.nttdocomo.co.jp) are with NTT DoCoMo, Inc., Yokosuka-shi, Kanagawa, Japan.

packet wireless access (hereafter, VSF-OFCDM) [7], which changes the spreading factor,  $SF$ , in both the time and frequency domains of OFCDM corresponding to the cell structure, channel load, propagation channel conditions, and major radio link parameters. Thus, through VSF-OFCDM, the seamless and flexible deployment of the same wireless access method both in multi-cell and isolated-cell environments is possible.

Using an actually implemented testbed, we previously reported on the average throughput of approximately 135 Mbps in a multipath fading channel using a 100 MHz bandwidth. Nevertheless, the achievable throughput of approximately 100 Mbps as the target of future wireless access schemes in around 2010 will not be sufficient considering the application to isolated-cell and indoor office environments, where an extremely large amount of traffic is concentrated in a limited short coverage area. Therefore, we set our target for the achievable peak throughput in these areas to approximately 1 Gbps, in contrast to that of more than 100 Mbps in a cellular system employing the identical air interface parameters such as frequency bandwidth, carrier frequency, duplex, wireless access, and frame structure. To achieve this high throughput, employing a space division multiplexing technique utilizing multiple antenna transmitters and receivers is inevitable, which is represented by the multiple-input multiple-output (MIMO) technique [8]-[11]. From the viewpoint of reducing the required average received signal energy per bit-to-background noise power spectrum density ratio ( $E_b/N_0$ ), we elucidated in [12] that MIMO multiplexing [8], [9], in which parallel coded data symbols are transmitted from each transmitter antenna branch, is superior to MIMO diversity such as space-time block coding [10], [11] and the adaptive antenna array beam forming transmitter associated with diversity reception to achieve a high frequency efficiency such as 10 bps/Hz, i.e., a 1 Gbps information bit rate using a 100 MHz bandwidth. This is because higher-level data modulation or a higher channel-coding rate than that in MIMO multiplexing must be used in MIMO diversity or the AAA-BF transmitter. Thereby, the number of data-decoding errors in the higher-level modulation with a shorter Euclidian distance and higher channel-coding rate is increased. Here, we consider that there are two major bottlenecks for the actual implementation of extremely high data-rate transceivers operating at the rate of 1 Gbps. The first issue is the de-multiplexing of the parallel data streams transmitted from  $N_{TX}$  transmitter antenna branches (here,  $N_{TX}$  is the number of transmitter antenna branches), which employ the same spreading code and frequency band within the identical time slot. Although the processing rates of the de-multiplexing of the parallel data streams from the  $N_{TX}$  transmitter antenna branches at the receiver are identical to that of a single antenna transmission, i.e., a  $1/N_{TX}$ -GHz-rate operation, a significantly

high level of computational complexity is needed especially for the application of the maximum likelihood detection (MLD)-based decoding (note that the required average received  $E_b/N_0$  applying the MLD is even superior to the minimum mean squared error (MMSE) or the Bell Labs layered space time method [8]). The second issue deals with the channel encoder and decoder, which are generally operated at 1 GHz to achieve a 1 Gbps data transmission by MIMO multiplexing. Therefore, implementing the channel decoder (turbo decoder, herein) becomes a bottleneck from the viewpoint of actual implementation.

This paper proposes a common interleaving method associated with independent channel-encoding among transmitter antenna branches in OFCDM-based MIMO multiplexing to achieve an extremely high throughput such as 1 Gbps using a 100 MHz bandwidth and investigates the achievable packet error rate (PER) performance in a multipath Rayleigh fading channel. Based on this simulation, we clarify that the proposed common interleaving method among transmitter antenna branches reduces the processing rate to  $1/N_{TX}$  in the turbo decoder, which is a bottleneck for implementing a 1 Gbps receiver, at the sacrifice of a slight loss in the required average received  $E_b/N_0$ . The rest of the paper is organized as follows. Section II first describes the proposed common interleaving and independent channel encoding among transmitter antenna branches along with the conventional common encoding and interleaving method and independent encoding and interleaving method. After describing the simulation configuration in section III, the simulation results are evaluated in section IV.

## II. Configurations for Independent Encoding and Common Interleaving Method

### 1. Conventional Encoding and Interleaving Method in MIMO Multiplexing

Before describing the proposed common interleaving and independent channel encoding method, we describe two conventional channel encoding and interleaving configurations in MIMO multiplexing.

#### A. Common Encoding and Interleaving Method

The configuration for the common channel encoding and interleaving method is illustrated in Fig. 1(a). The original transmitted data sequence is first channel encoded and data modulation mapping is performed, followed by symbol interleaving in the frequency and space domains. The coded data sequence is serial-to-parallel-converted into  $N_{TX}$  parallel sequences corresponding to the number of transmission

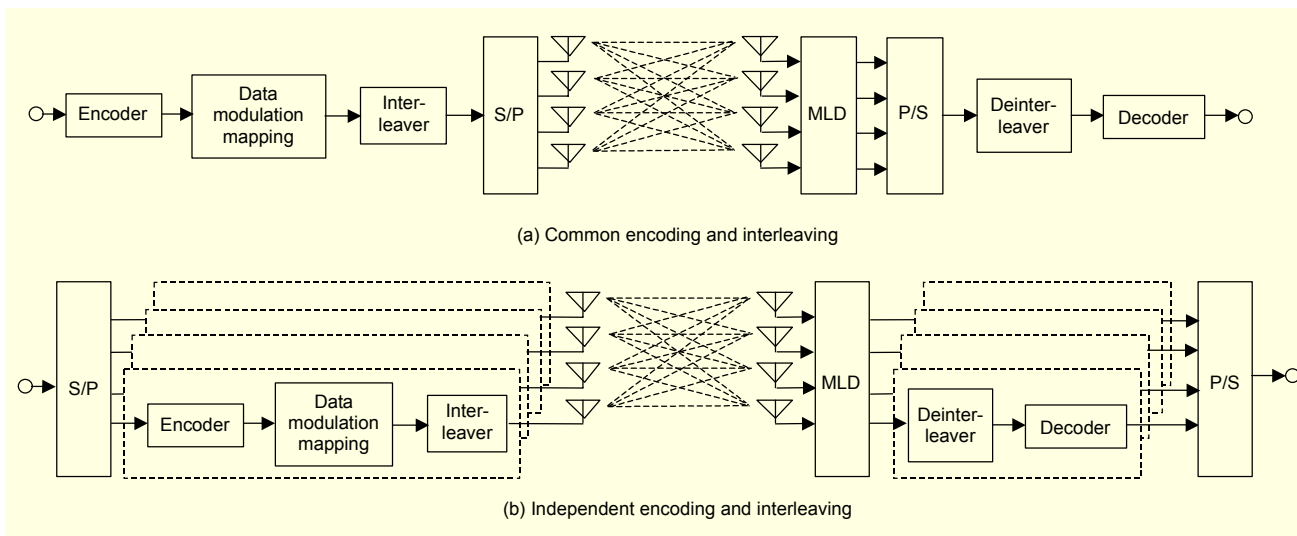


Fig. 1. Conventional configuration of encoding and interleaving.

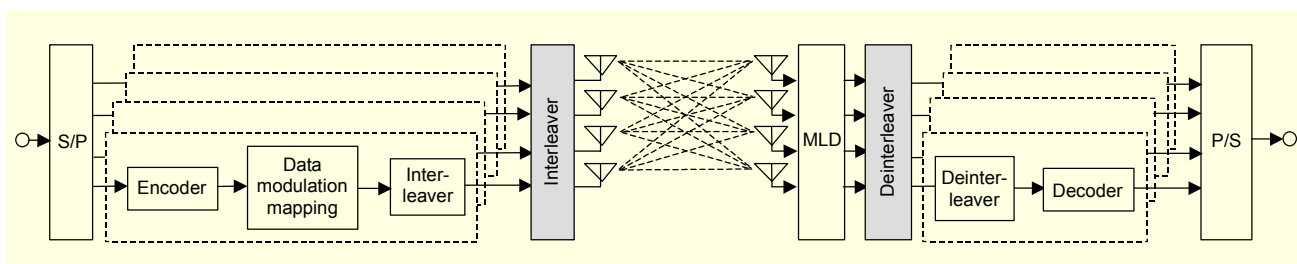


Fig. 2. Proposed configuration of encoding and interleaving (Independent encoding and common interleaving).

antenna branches, followed by the multiplexing of pilot symbols used for channel estimation associated with each of the transmitted  $N_{TX}$  data streams and OFCDM signal generation. The coded data sequence at each transmitter antenna branch is serial-to-parallel-converted again into  $N_{sub}$  sub-carrier streams, and inverse fast Fourier transform (IFFT) processing is performed to generate a multi-carrier signal. This is followed by the insertion of a guard interval (prefix) to avoid inter-symbol interference.

At the receiver, the  $N_{sub}$  sub-carrier signal is first converted into a parallel data sequence by FFT processing (in the paper, we assume ideal OFCDM symbol timing detection). The transmitted data sequences from  $N_{TX}$  antenna branches are de-multiplexed from the received composite signal at  $N_{RX}$  antenna branches based on the MLD algorithm employing the estimated channel impulse response, i.e., channel gain by pilot channel-assisted channel estimation. In MLD, metric  $d$  defined in (1) is calculated for all replica candidates of the transmitted data modulation phase and amplitude associated with the  $i$ -th ( $1 \leq i \leq N_{TX}$ ) transmitter antenna branch,  $c_i$ , by using the received signal at the  $j$ -th ( $1 \leq j \leq N_{RX}$ ) antenna branch,  $r_j$ , and estimated channel gain between the  $i$ -th transmitter antenna

branch and the  $j$ -th receiver antenna branch,  $h_{i,j}$ .

$$d = \sum_{j=1}^{N_{RX}} \left| r_j - \sum_{i=1}^{N_{TX}} h_{i,j} c_i \right|^2. \quad (1)$$

Thus, the transmitted data modulation phase and amplitude associated with the  $i$ -th transmitter antenna branch,  $c_i$ , is simultaneously obtained based on the selection of the transmitted data modulation phase and amplitude, which minimizes the metric among the metrics of all replica candidates. After each de-multiplexed data sequence is parallel-to-serial converted, de-interleaving and turbo decoding are performed to recover the transmitted information data sequence in the method.

### B. Independent Encoding and Interleaving Method

Figure 1(b) shows the configuration for the independent channel encoding and interleaving method. The original transmitted data sequence is first serial-to-parallel converted into  $N_{TX}$  parallel sequences corresponding to the number of transmitter antenna branches. The data sequence with rate

$1/N_{TX}$ , which is lower than that of the original information bit rate, is channel encoded, and after data modulation mapping, interleaving is performed in the frequency domain. The coded data sequence is serial-to-parallel converted again into  $N_{sub}$  sub-carrier streams, and IFFT processing is performed to generate a multi-carrier signal. This is followed by the insertion of a guard interval. At the receiver, similar to method (a) in Fig. 1, FFT processing is first performed to generate parallel  $N_{sub}$  sub-carrier signals, followed by MLD. The de-multiplexed symbol sequence in MLD associated with the transmitter antenna branch is de-interleaved and turbo decoded independently. Finally, the decoded bit sequence is parallel-to-serial converted to recover the original information bit sequence.

## 2. Proposed Common Interleaving and Independent Encoding Method

In the proposed common interleaving method associated with independent channel encoding as shown in Fig. 2, the original transmitted data sequence is first serial-to-parallel converted into  $N_{TX}$  parallel sequences corresponding to the number of transmitter antenna branches and independently channel-encoded. Data-modulation mapping is independently performed for the coded bit sequence. Subsequently, the  $N_{TX}$ -encoded symbol sequence is interleaved in the frequency and space domains. The  $N_{TX}$  symbol sequence after interleaving is serial-to-parallel converted again into  $N_{sub}$  sub-carrier streams independently, and IFFT processing is performed to generate a multi-carrier signal. This is followed by the insertion of a guard interval. At the receiver, the processing by FFT and MLD are identical to those in methods (a) and (b) in Fig. 1. After the de-multiplexed data sequence is de-interleaved, the  $N_{TX}$  symbol sequence is turbo decoded followed by parallel-to-serial conversion to recover the original information bit sequence. Note that by employing the common interleaving method as shown in Fig. 2, the operation (i.e., reading and writing) speed into/from the buffer memory circuitry is identical to that with a single antenna transmission, because writing and reading operations are simultaneously performed among  $N_{TX}$  and  $N_{RX}$  antenna branches. However, in the proposed method, we can expect an averaging effect of the received signal level among receiver antenna branches, bringing about improvement derived from the channel coding effect.

## III. Simulation Configuration

The frame format and simulation parameters are given in Fig. 3 and Table 1, respectively. We assume an  $N_{sub} = 768$  sub-carrier OFCDM signal along with the carrier separation of 131 kHz resulting in a total bandwidth of 101.5 MHz. The frame

length is 0.48 ms. We use Turbo coding with a coding rate of 1/3 and a constraint length of four bits, and higher coding rates such as  $R = 5/6$  are generated by puncturing the 1/3-rate code.

The configurations of the OFCDM signal processing block in the transmitter and receiver are illustrated in Figs. 4(a) and 4(b), respectively. At the transmitter, binary information data bits are encoded by turbo coding and data modulated, then the encoded data sequence stream is symbol interleaved based on the scheme in [13]. After serial-to-parallel conversion into  $N_{sub} = 768$  sub-carrier OFCDM symbols (the effective symbol duration is  $7.585 \mu\text{s}$  corresponding to 1024 FFT samples) using IFFT, the coded data symbol sequence is spread by the spreading factor combination of  $SF_{Time} = 4$  and  $SF_{Freq} = 1$  ( $SF_{Time}$  and  $SF_{Freq}$  are the spreading factors in the time and frequency domains, respectively). This is followed by pilot symbol multiplexing for channel estimation at the receiver.

We employ orthogonal pilot symbol patterns for  $N_{TX}$  antenna branches. In order to avoid inter-symbol interference caused by multipath propagation, a guard interval with a length of  $1.674 \mu\text{s}$  corresponding to 226 FFT samples is inserted between the

Table 1. Simulation parameters.

Bandwidth		101.5 MHz
Number of sub-carriers, $N_{sub}$		768
OFDM symbol duration	Data	7.585 $\mu\text{s}$
	Guard interval	1.674 $\mu\text{s}$
Spreading factor		$SF_{Time}=4$ and $SF_{Freq}=1$
Number of multiplexing codes		4
Packet length	Data	48 symbols
	Pilot	4 symbols
Modulation		16QAM
Channel coding/decoding		<ul style="list-style-type: none"> <li>• Turbo code</li> <li>- Coding rate = 5/6</li> <li>- Constraint length = 4</li> <li>• Max-Log-MAP decoding (Iterations = 8)</li> </ul>
Channel estimation		Pilot symbol assisted channel estimation
Number of antenna branches	Transmitter, $N_{TX}$	4
	Receiver, $N_{RX}$	2, 3, and 4
Information bit rate		983 Mbps
Channel model		<ul style="list-style-type: none"> <li>• Exponential decayed L=1, 6, 12-path Rayleigh</li> <li>• Maximum Doppler frequency: <math>f_D = 20</math> Hz</li> </ul>
rms delay spread ( $\sigma$ )		0, 0.17, 0.34, and 0.52 $\mu\text{s}$
Fading correlation factor ( $\rho$ )		0, 0.2, 0.4, 0.6, 0.8, and 1.0

OFCDM symbols. The resultant frame comprises 52 OFCDM symbols.

We assume an  $L$ -path exponentially-decayed Rayleigh fading channel model with a fading maximum Doppler frequency of  $f_D = 20$  Hz. For  $L = 6$  and 12, the average received signal power is reduced by 1 dB in decreasing order starting from the first path, with the root mean squared (rms) delay spread as a parameter from  $\sigma = 0$  to  $0.52 \mu\text{s}$  (note that in this case, the maximum time delay becomes approximately  $2.0 \mu\text{s}$ ).

At the receiver, after the guard interval is removed, 768 parallel data sequences are de-multiplexed by FFT processing from the multicarrier signal with 768 sub-carriers. The channel gain of each frame associated with each propagation channel at

each sub-carrier is estimated by coherently accumulating four pilot symbols within a frame, since different orthogonal pilot symbol patterns are used for each data stream corresponding to each transmitter antenna branch. The spread sequence at each sub-carrier is despread in the time domain. In the MLD algorithm used in MIMO multiplexing, we select the optimum replica yielding the minimum mean squared error among all the constellation candidates, which is generated based on the estimated channel gain for each sub-carrier. After demultiplexing into parallel data streams corresponding to each transmitter antenna branch, the resultant sequences are parallel-to-serial converted and turbo decoded by the Max-Log-MAP algorithm with eight iterations to recover the transmitted binary data.

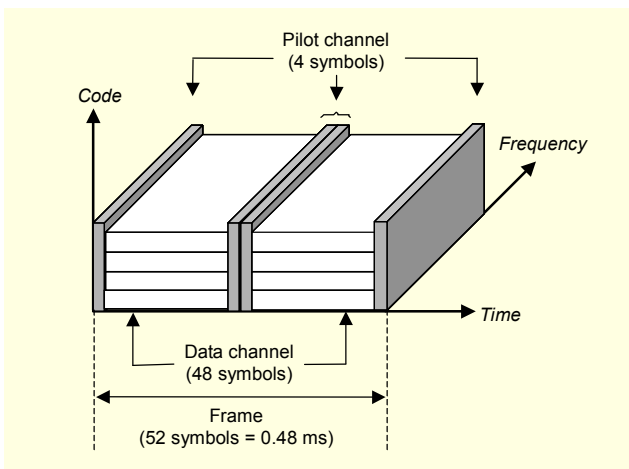


Fig. 3. Frame format.

#### IV. Simulation Results

The average PER performance at the information bit rate of 983 Mbps is plotted in Fig. 5 as a function of the average received  $E_b/N_0$  with  $N_{TX} = N_{RX} = 4$  for the fading maximum Doppler frequency of  $f_D = 20$  Hz. Figures 5(a), 5(b), and 5(c) show the PER performance for the number of paths of  $L = 1, 6,$  and  $12$ , respectively. The rms delay spread values for  $L = 1, 6,$  and  $12$  are  $0.0, 0.17,$  and  $0.34 \mu\text{s}$ , respectively. The fading correlations among  $N_{TX} = 4$  transmitter antenna branches and those among  $N_{RX} = 4$  receiver antenna branches are assumed to be  $\rho = 0$ . We clearly see that there is no error floor and that Figs. 5(a) to 5(c) indicate the possibility of a 1 Gbps information bit rate based on the radio parameters with a bandwidth of 100 MHz.

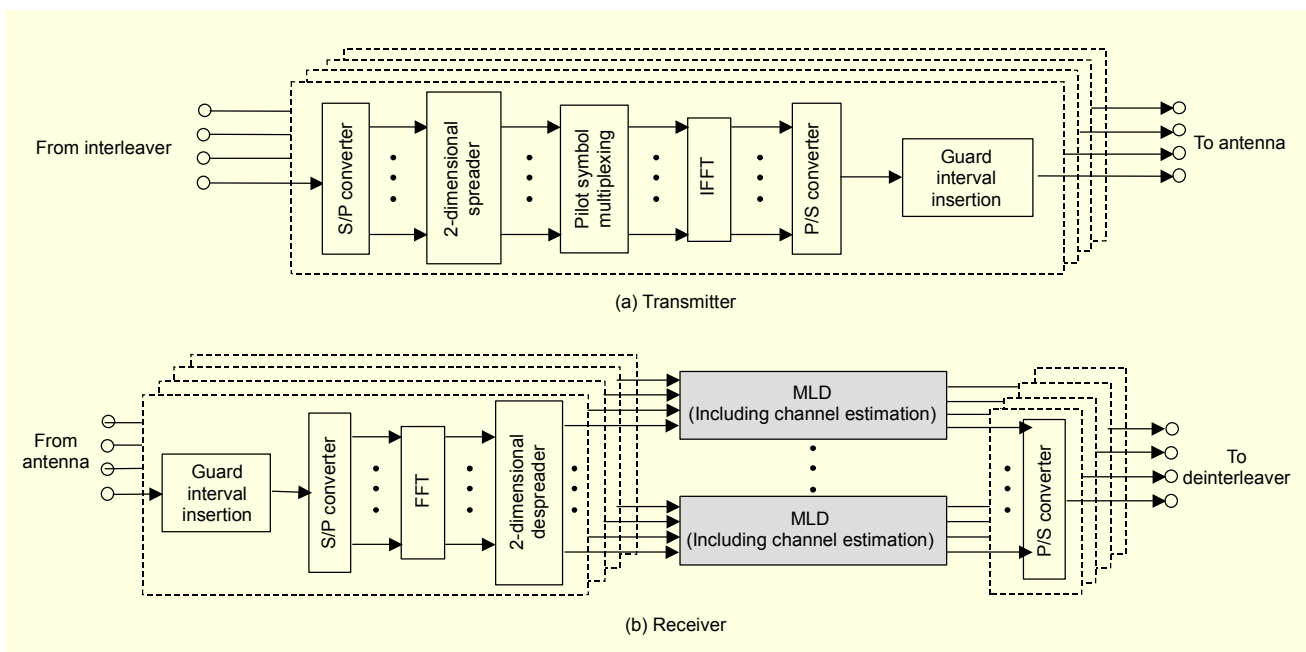


Fig. 4. OFCDM signal processing.



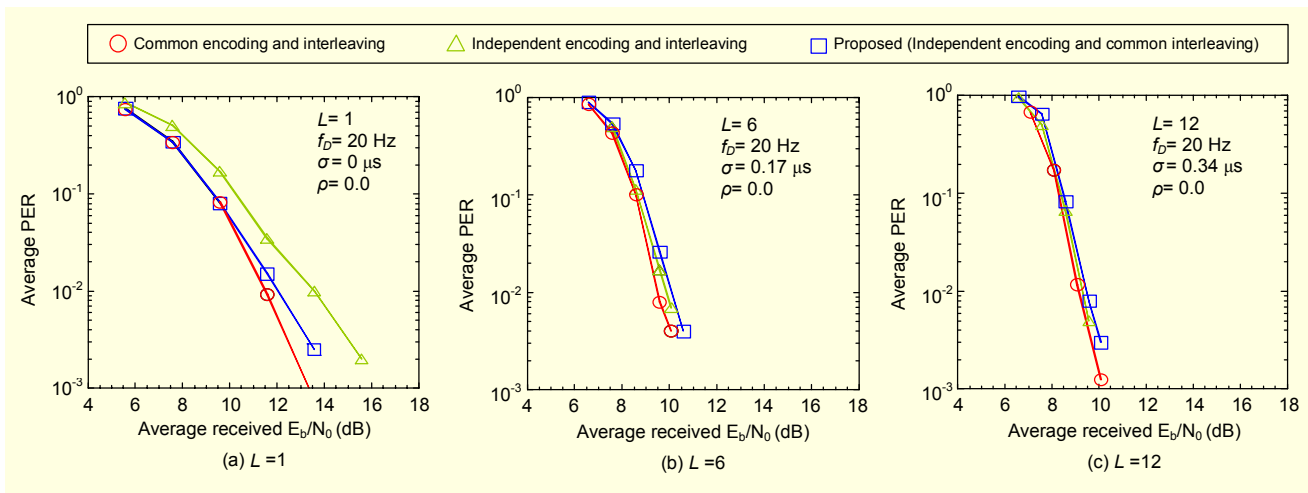


Fig. 5. Average PER performances of (a)  $L = 1$ , (b)  $L = 6$ , and (c)  $L = 12$ .

Figure 5(a) shows that the common encoding and interleaving method reduces the required average received  $E_b/N_0$  at the average PER of  $10^{-2}$  by approximately 2.0 dB compared to that using the independent encoding and interleaving method. This is because a large turbo coding effect is gained by interleaving over  $N_{TX}$  transmitter antenna branches. Nevertheless, we find that the loss in the required average received  $E_b/N_0$  of the proposed independent encoding and common interleaving method from the common encoding and interleaving method is slight, while the processing rate in the turbo decoder can be decreased to 1/4. This result suggests that a sufficient randomization effect in the received signal level is gained by only interleaving among  $N_{TX}$  antenna branches. Next, by comparing the PER performance in Fig. 5(b) to that in Fig. 5(a), we find that the degradation in the required average received  $E_b/N_0$  using the independent encoding and interleaving method from that with the common encoding and interleaving method for  $L = 6$  is less than that for  $L = 1$ . This is because as the  $L$  value increases from 1 to 6, the variation in the received signal level due to fading over the  $N_{TX}$  data streams is reduced by the frequency diversity effect. Moreover, Fig. 5(c) shows that when  $L$  is 12, no distinct difference in the PER performance of the three methods is observed, since the fluctuation in the received signal level is more sufficiently randomized by further increasing the  $L$  value. Thus, we can find that in the frequency-selective fading channel with  $L = 1$  to  $L = 12$ , the loss in the required average received  $E_b/N_0$  at the average PER of  $10^{-2}$  using the proposed independent encoding and common interleaving method compared to that with the common encoding and interleaving method is very small, i.e., within approximately 0.3 dB.

The average received  $E_b/N_0$  at the average PER of  $10^{-2}$  is plotted in Fig. 6 as a function of the rms delay spread,  $\sigma$ , for  $L$

$= 12$ ,  $f_D = 20$  Hz, and  $\rho = 0$ . We set  $N_{TX} = N_{RX} = 4$  in the figure. Figure 6 shows that the loss in the required average received  $E_b/N_0$  using the proposed method from that using the common encoding and interleaving method is slight regardless of  $\sigma$ . Meanwhile, the required average received  $E_b/N_0$  value employing the independent encoding and interleaving method for  $\sigma = 0$  is degraded by approximately 2.0 dB compared to that using the common encoding and interleaving method or the proposed independent encoding and common interleaving method. As shown in the figure, according to the increase in the  $\sigma$  value from 0, the required average received  $E_b/N_0$  is first reduced owing to the increasing frequency diversity effect, i.e., the increasing randomization effect in the fluctuation of the received signal level over different data streams from  $N_{TX} = 4$  antenna branches. Nevertheless, it is conversely increased beyond the  $\sigma$  of approximately 0.2  $\mu$ s, because the paths, which exceeded the guard interval length, are increased.

As is well known, accurate separation of the composite received signal transmitted from  $N_{TX} = 4$  antenna branches in the MLD processing strongly depends on the fading correlation among antenna branches,  $\rho$ . Thereby, the value of  $\rho$  affects the achievable required average received  $E_b/N_0$  performance. Thus, the average received  $E_b/N_0$  at the average PER of  $10^{-2}$  as a function of the  $\rho$  value is plotted in Fig. 7 for  $L = 12$ ,  $f_D = 20$  Hz, and  $\sigma = 0.34$   $\mu$ s, associated with  $N_{TX} = N_{RX} = 4$ . In the evaluation results shown in Fig. 7, we assumed that both the fading correlations among transmitter antenna branches and those among receiver antenna branches were  $\rho$ . Figure 7 shows that there are no obvious differences in the required average received  $E_b/N_0$  among the three methods. Moreover, according to the increase in  $\rho$ , the required average received  $E_b/N_0$  is increased since the errors in the generated constellation replicas based in the estimated channel gains are increased. However,

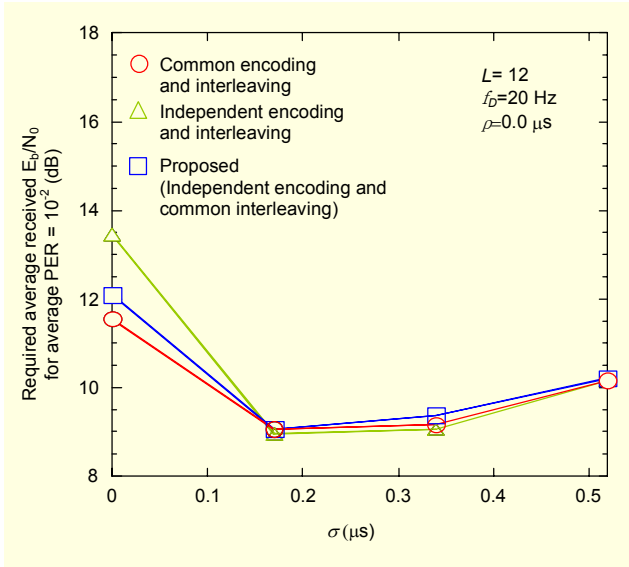


Fig. 6. Influence of rms delay spread,  $\sigma$ .

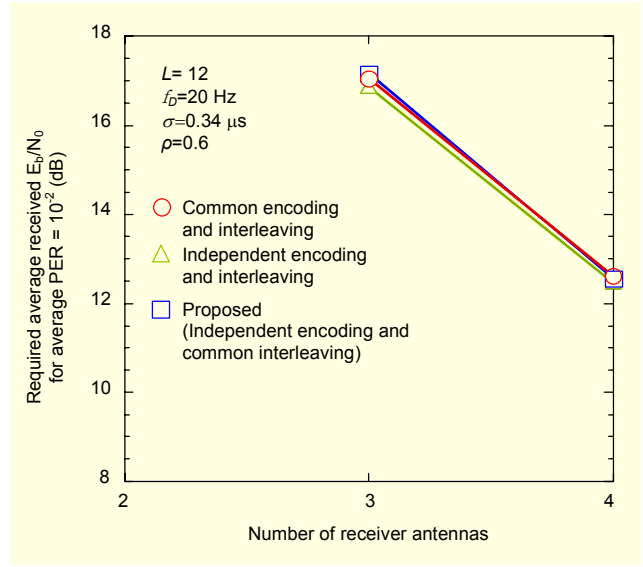


Fig. 8. Required average received  $E_b/N_0$  for an average PER of  $10^{-2}$  as a function of the number of receiver antenna branches,  $N_{RX}$ .

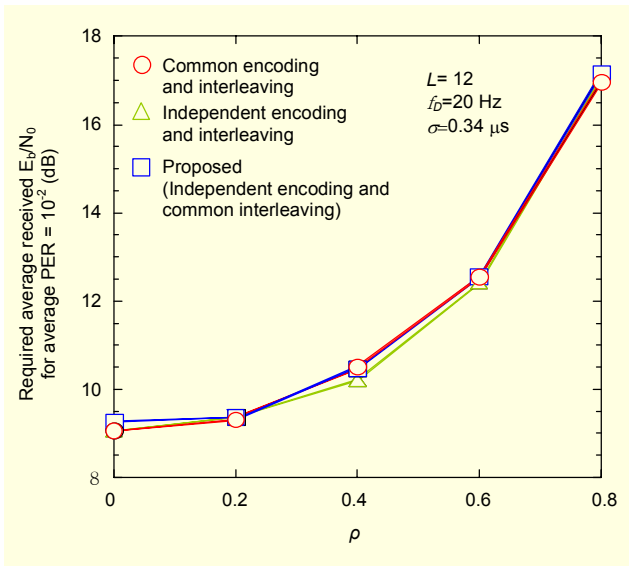


Fig. 7. Influence of fading correlation factor,  $\rho$ .

the results in Fig. 7 indicate that even for a large  $\rho$  value such as 0.8, the information bit rate of almost 1 Gbps is still possible by increasing the transmission power.

Thus far, we assumed  $N_{RX} = 4$  in regard to  $N_{TX} = 4$ . So, the average received  $E_b/N_0$  at the average PER of  $10^{-2}$  as a function of the  $N_{RX}$  value is plotted in Fig. 8 for  $N_{TX} = 4$  assuming  $L = 12$ ,  $f_D = 20$  Hz,  $\sigma = 0.34$   $\mu\text{s}$ , and  $\rho = 0.6$ . When  $N_{RX}$  is 2, we cannot achieve the average PER of  $10^{-2}$ . As shown in Fig. 8, the required average received  $E_b/N_0$  for  $N_{RX} = 4$  is reduced by approximately 4 dB compared to that for  $N_{RX} = 3$ , because the mean squared error between the received composite signal and constellation candidates is further refined by averaging over a

large number of receiver antenna branches.

Finally, we discuss the computational complexity of the turbo decoding compared to that for signal separation based on MLD. First, from [14], the required number of real multiplications for MLD assuming  $4 \times 4$  MIMO multiplexing and 16QAM data modulation to achieve a 1 Gbps data rate becomes approximately  $1.9 \times 10^{10}$  per 0.5 ms frame. Furthermore, if we use the complexity reduced MLD called QRM-MLD [14], [15], which utilizes QR decomposition of the channel matrix and the M-algorithm, the required number of real multiplications is reduced to approximately  $6.1 \times 10^7$  while suppressing the loss in the required average received  $E_b/N_0$  from the conventional MLD within approximately 0.5 dB. Note that although signal separation also requires other operations such as addition and division, the dominant portion of the total complexity is on real multiplications. On the other hand, from [16], the required number of equivalent real additions in turbo decoding per 0.5 ms frame becomes approximately  $8.2 \times 10^8$ , assuming a 1 Gbps data rate, Max-Log-MAP decoding with eight iterations, and the constraint length of four bits. Note that the computational complexity of symbol interleaving for both cases with transmit antenna-independent and common methods can be much smaller than that for MLD and turbo decoding, since the required operations of symbol interleaving comprise one write operation to the memory and one read operation from the memory per symbol. Assuming that the calculation cost of real multiplication is ten times higher than that of real addition, the calculation cost (computational complexity) of turbo decoding is approximately 1.3 times that of the complexity-reduced MLD

(QRM-MLD). Therefore, the reduction in the processing rate to 1/4 in the turbo decoder by using the proposed common interleaving and independent channel-encoding method is expected to be very beneficial for implementing a 1 Gbps receiver.

## V. Conclusion

This paper proposed a common interleaving method associated with independent channel encoding among transmitter antenna branches in OFCDM MIMO multiplexing to achieve an extremely high throughput such as 1 Gbps using a 100 MHz bandwidth and investigated the achievable PER performance in multipath Rayleigh fading channels. The simulation results elucidated that with four-branch MIMO multiplexing, the loss in the required average received  $E_b/N_0$  of the proposed independent encoding and common interleaving method compared to that of the conventional common encoding and interleaving method was only approximately 0.3 dB in a multipath fading channel of up to 12 paths with a fading maximum Doppler frequency of  $f_D = 20$  Hz, using the combination of 16QAM modulation and a coding rate of 5/6. It was also clarified that even for a large fading correlation among antenna branches such as 0.8, an information bit rate of almost 1 Gbps was still possible by increasing the required transmission power. Therefore, the proposed common interleaving and independent channel encoding method among transmitter antenna branches reduced the processing rate to 1/4 in the turbo decoder, which is a bottleneck for implementing a 1 Gbps receiver, at the sacrifice of a slight loss in the required received  $E_b/N_0$ .

## References

- [1] 3GPP, 3GTR25.848, *Physical Layer Aspects of UTRA High Speed Downlink Packet Access*, Mar. 2001.
- [2] H. Atarashi, S. Abeta, and M. Sawahashi, "Broadband Packet Wireless Access Appropriate for High-Speed and High-Capacity Throughput," *IEEE VTC2001-Spring*, vol. 1, May 2001, pp. 566-570.
- [3] S. Abeta, H. Atarashi, M. Sawahashi, and F. Adachi, "Performance of Coherent Multi-Carrier/DS-CDMA and MC-CDMA for Broadband Packet Wireless Access," *IEICE Trans. Commun.*, vol. E84-B, no. 3, Mar. 2001, pp. 415-424.
- [4] S. Abeta, H. Atarashi, and M. Sawahashi, "Forward Link Capacity of Coherent DS-CDMA and MC-CDMA Broadband Packet Wireless Access in a Multi-Cell Environment," *IEEE VTC2000-Fall*, Boston, Sept. 2000, pp. 2213-2218.
- [5] N. Yee, J.-P. Linnartz, and G. Fettweis, "Multi-Carrier CDMA in Indoor Wireless Radio Networks," *IEEE PIMRC'93*, Sept. 1993, pp. 109-113.
- [6] K. Fazel and L. Papke, "On the Performance of Convolutional-Coded CDMA/OFDM for Mobile Communication Systems," *IEEE PIMRC'93*, Sept. 1993, pp. 468-472.
- [7] H. Atarashi, S. Abeta, and M. Sawahashi, "Variable Spreading Factor-Orthogonal Frequency and Code Division Multiplexing (VSF-OFCDM) for Broadband Wireless Access," *IEICE Trans. Commun.*, vol. E86-B, no. 1, Jan. 2003, pp. 291-299.
- [8] G.J. Foschini Jr., "Layered Space-Time Architecture for Wireless Communication in a Fading Environment When Using Multi-Element Antennas," *Bell Labs Tech. J.*, Autumn 1996, pp. 41-59.
- [9] H. Bolcskei, D. Gesbert, and A.J. Paulaj, "On the Capacity of OFDM-Based Special Multiplexing Systems," *IEEE Trans. Commun.*, vol. 50, Feb. 2002, pp. 225-234.
- [10] V. Tarokh, H. Jafarkhani, and R. Calderbank, "Space-Time Block Coding for Wireless Communications: Performance Results," *IEEE J. Select. Areas Commun.*, vol. 17, no. 3, Mar. 1999, pp. 451-460.
- [11] S.M. Alamouti, "A Simple Transmit Diversity Technique for Wireless Communications," *IEEE J. Select. Areas Commun.*, vol. 16, no. 8, Oct. 1998, pp. 1451-1458.
- [12] J. Kawamoto, T. Asai, K. Higuchi, and M. Sawahashi, "Comparison of Space Division Multiplexing Schemes Employing Multiple Antennas in OFDM Forward Link," *IEEE VTC2003-Fall*, Oct. 2003.
- [13] N. Maeda, H. Atarashi, and M. Sawahashi, "Performance Comparison of Channel Interleaving Methods in Frequency Domain for VSF-OFCDM Broadband Wireless Access in Forward Link," *IEICE Trans. Commun.*, vol. E86-B, no. 1, Jan. 2003, pp. 300-313.
- [14] H. Kawai, K. Higuchi, N. Maeda, M. Sawahashi, T. Itoh, Y. Kakura, A. Ushirokawa, and H. Seki, "Likelihood Function for QRM-MLD Suitable for Soft-Decision Turbo Decoding and its Performance for OFCDM MIMO Multiplexing in Multipath Fading Channel," submitted to *IEICE Trans. Commun.*
- [15] K.J. Kim and J. Yue, "Joint Channel Estimation and Data Detection Algorithms for MIMO-OFDM systems," *Thirty-Sixth Asilomar Conf. Signals, Systems and Computers*, Nov. 2002, pp. 1857-1861.
- [16] P.H.Y. Wu, "On the Complexity of Turbo Decoding Algorithms," *IEEE VTC 2001-Spring*, vol. 2, 6-9 May 2001, pp. 1439-1443.





**Junichiro Kawamoto** received the BS and MS degrees from Tsukuba University, Tsukuba, Japan, in 1999 and 2001. In 2002, he joined NTT DoCoMo, Inc. Since joining NTT DoCoMo, Inc., he has been engaged in the research and development of MIMO systems.



**Takahiro Asai** received the BS and MS degrees from Kyoto University, Kyoto, Japan, in 1995 and 1997. In 1997, he joined NTT Mobile Communications Network, Inc. (now NTT DoCoMo, Inc.). Since joining NTT Mobile Communications Network, Inc., he has been engaged in the research and development

of mobile radio systems.



**Kenichi Higuchi** received the BS degree from Waseda University, Tokyo, Japan, in 1994, and received his Dr. Eng. degree from Tohoku University, Sendai, Japan, in 2002. In 1994, he joined NTT Mobile Communications Network, Inc. (now, NTT DoCoMo, Inc.). Since joining

NTT Mobile Communications Network, Inc., he has been engaged in the research and development of a code synchronization and interference canceller technique for wideband DS-CDMA mobile radio systems and an adaptive antenna array technique for broadband wireless packet access.



**Mamoru Sawahashi** received the BS and MS degrees from Tokyo University in 1983 and 1985, and received the Dr. Eng. degree from the Nara Institute of Technology in 1998. In 1985, he joined NTT Electrical Communications Laboratories, and in 1992 he transferred to NTT Mobile Communications Network, Inc. (now,

NTT DoCoMo, Inc.). Since joining NTT, he has been engaged in the research of modulation/demodulation techniques for mobile radio, and the research and development of wireless access technologies for W-CDMA mobile radio and broadband wireless packet access technologies for beyond IMT-2000. He is now the Director of the Radio Access System Group in the IP Radio Network Development Department of NTT DoCoMo, Inc.